Sains Malaysiana 41(6)(2012): 761–768

Electrical and Magneto-Transport Properties of Magneto-Resistive $La_{0.7}Ca_{0.28}Sr_{0.2}MnO_3$ Prepared at Different Sintering Temperature

(Sifat Elektrik dan Magneto-Angkutan $La_{0.7}Ca_{0.28}Sr_{0.2}MnO_3$ yang disediakan pada Suhu Sinteran Berlainan)

L.S. EWE,* R. RAMLI, K.P. LIM & R. ABD-SHUKOR

ABSTRACT

The effects of strontium doping on the electrical and magneto-transport properties of magneto resistive $La_{0.7}Ca_{0.28}Sr_{0.02}MnO_3$ at different sintering temperatures have been studied. The samples were prepared by the co-precipitation technique (COP) and sintered at 1120, 1220 and 1320 °C. XRD patterns revealed that the samples have an orthorhombic structure and the diffraction patterns can be indexed with the Pbnm space group. The insulator metal transition, T_{IM} increased linearly from 261 K to 272 K with the increase in sintering temperature. The magnetoresistance (MR) measurements were made in magnetic fields from 0.1 to 1 T at room temperature. The percentage of MR increased with increasing of magnetic field and sintering temperature for all samples. The electrical resistivity data were fitted with several equations in the metallic (ferromagnetic) and insulator (paramagnetic) regime. The density of states at the Fermi level $N(E_F)$ and the activation energy (E_a) of electron hopping were estimated by using variable range hopping and small polaron hopping model.

Keywords: Activation energy; electrical resistivity; magnetotransport; manganites

ABSTRAK

Kesan pengedopan strontium terhadap sifat elektrik dan magneto angkutan bahan magneto rintangan $La_{0.7}Ca_{0.28}Sr_{0.02}MnO_3$ yang disediakan pada suhu sinteran berlainan telah dikaji. Sampel telah disediakan dengan kaedah co-pemendakan (COP) dan disinter pada 1120, 1220 and 1320 °C. Corak XRD menunjukkan semua sampel mempunyai struktur ortorombik dan corak pembelauan boleh diindeks kepada kumpulan ruang Pbnm. Peralihan penebat logam T_{IM} meningkat secara linear daripada 261 hingga 272 K dengan peningkatan suhu sinteran. Pengukuran magneto rintangan (MR) telah dijalankan dalam medan magnet daripada 0.1 hingga 1 T pada suhu bilik. Peratusan peningkatan MR meningkat dengan medan magnet dan suhu sinteran untuk semua sampel. Data kerintangan elektrik telah disuaikan dengan beberapa model dalam rantau logam (feromagnet) dan penebat (paramagnet). Ketumpatan keadaan pada aras Fermi $N(E_F)$ dan tenaga pengaktifan (E_a) loncatan elektron telah dijangkakan dengan menggunakan model loncatan julat berubah dan model polaron kecil.

Kata kunci: Kerintangan elektrik; magneto rintangan; manganit; tenaga pengaktifan

INTRODUCTION

The interest in perovskite manganites with the form $A_xB_{1-x}MnO_3$ (A is typically a trivalent rare-earth and B is a divalent alkaline) in recent years was due to colossal magnetoresistance effect (CMR) in this material and the potential applications in magnetoresistive transduser and magnetic sensors (Xiong et al. 2009). The oxygen in these materials has a filled outer shell (2p) being in the O^{2-} state. Mn presents in two oxidation states Mn^{4+} and Mn^{3+} and the compound is in the mixed state of $A^{3+}_{1-x}B^{2+}_xMn^{3+}_{1-x}Mn^{4+}_xO^{2-}_3$. In order to get charge neutrality, the ratio Mn^{3+}/Mn^{4+} is equal to the ratio A^{3+}/B^{2+}. Therefore doping with B equivalent can change the valence of the Mn ions from +3 to +4 (Rao & Raychaudhuri 1998). Mn^{4+} lacks of e_g electron and hence the itinerant hole associated with the Mn^{4+} ions may hop to Mn^{3+}. However, because of the strong on-site exchange interaction (Hund's rule) with the localized Mn electrons, only hoping between sites with localized parallel spins is favored (Venkataiah & Venugopal 2005). This is the essence of double exchange model and is used to explain the physical nature of the interaction and the simultaneous occurrence of ferromagnetism and metallic nature of the material below the insulator-metal transition temperature (T_{IM}). The overlap of O p- and Mn d- orbital depends on the Mn-Mn distance and Mn-O-Mn angle that can be modified by varying the average size of ions at Mn site (Rao & Raychaudhuri 1998).

The manganites doped with calcium and strontium (Karmakar et al. 2005; Ravi et al. 2007; Roul et al. 2001; Venkataiah et al. 2007; Zainullina et al. 2004; Zhang et al. 2002) received much attention due to the high T_c and small variance of the B site ionic radii. Recent studies on these materials revealed that CMR phenomenon is attributed not only to the double exchange (DE) mechanism but also to the interactions such as electron-phonon coupling, electron-magnon interaction, and the complicated band structure

(Venkataiah & Venugopal 2005). With the increase in annealing temperature of nanocrystalline ferromagnetic $La_{0.7}Sr_{0.06}Ca_{0.24}MnO_3$ perovskites, the grain size and insulator-metal transition temperature (T_{IM}) increases, and the magnetoresistance (MR) effect at 77 K decreases (Jin et al. 1994). Furthermore, $La_{0.67}Ca_{0.33-x}Sr_xMnO_3$ up to $x = 0.13$ exhibit orthorhombic structure with Pbnm space group [14]. The T_{IM} for $La_{0.67}Ca_{0.33}MnO_3$ sintered at different temperature is almost constant (~271 K) and MR is almost constant in 0.5 and 1 T applied fields between 200 and 250 K (Ewe et al. 2009).

Venkataiah et al. (2007) have reported that the T_o values decreases with an increase in the sintering temperature in $La_{0.67}Ca_{0.33}MnO_3$. T_o can be calculated using the well known relation $T_0 = \frac{16\alpha^3}{k_B N(E_F)}$, where α is the length of localized electron in the paramagnetic state and is considered as 2.22 nm^{-1} and $N(E_F)$ is the density of states at the Fermi level (Chattopadhyay et al. 2007). According to Fontcuberta et al. 1996, the increase in T_o value is due to the bending of Mn-O-Mn bond and hence it reflects the enhancement of carrier effective mass or narrowing of the bandwidth, which in turn results in a drastic change in the resistivity peak in the vicinity of T_{IM}. Increase of sintering temperature induced the formation of an interfacial phase near the grain boundaries in $La_{0.67}Sr_{0.33}MnO_3$ and $Nd_{0.67}Sr_{0.33}MnO_3$ (Chang & Ong 2004).

The microstructure, magnetic and electrical properties of the material strongly depend on the starting crystallites size (Grossin & Noudem 2004). Dagotto et al. (2001) have also reported that $La_{0.67}Ca_{0.33}MnO_3$ exhibits high magnetoresistance and $La_{0.67}Sr_{0.33}MnO_3$ exhibits high magnetic transition temperature T_c,. In view of these results, it is interesting to study the effect a small amount of strontium doping in B sites on the electrical and magnetotransport properties of LCMO. In this paper we report the results of a study on $La_{0.7}Ca_{0.28}Sr_{0.02}MnO_3$ (LCSMO) sintered at different temperatures.

Experimental Details

The co-precipitation method was used to prepare polycrystalline samples of composition $La_{0.7}Ca_{0.28}Sr_{0.02}MnO_3$. Appropriate amounts of lanthanum acetate, calcium acetate, strontium acetate and manganese acetate (purity ≥ 99.9%) were weighted, mixed and then dissolved in glacial acetate acid. Oxalic acid (0.5 M) was added to the solution in an ice bath until a white suspension was amassed. The resulting slurry was filtered after 5 min of reaction and dried in an oven at 80 °C for 8 h. The powders were then calcined at 900 °C in air for 12 h. The resulting powders were then pressed into pellets and sintered at 1120, 1220 and 1320 °C.

The phase purity of the samples were examined by the X-ray diffraction (XRD) method using a Siemens D5000 diffractometer with CuK_α radiation (λ = 1.5418 Å). The surface morphology was recorded by a scanning electron microscope (SEM). The temperature dependence of the electrical resistivity was studied in the temperature range of 50 - 300 K in zero field using the standard four probe method. The MR measurement system consists of a magnetic coil with high voltage current power supply, a gauss meter (F.W.Bell, model 5080), a four probe point holder, DC voltage current supply (Yew type 2553), and a Keithley 197A auto-raging microvoltmeter. The change in sample resistance was measured with a known constant current in 0.1 – 1 T fields at room temperature.

The average grain size was estimated using the intercept method. The theoretical density ϱ_{th} was determined by dividing the mass per unit cell by the volume of the unit cell. The volume of the unit cell was calculated from the lattice parameters obtained from XRD data. The experimental density ϱ_{exp} was calculated by dividing the mass of the sample with the volume obtained geometrically. By using the theoretical and measured density, the porosity was calculated by using the equation, $\text{Porosity}(\%) = \frac{\rho_{th} - \rho_{exp}}{\rho_{th}} \times 100\%$

Results and Discussion

The x-ray diffraction patterns (Figure 1) showed that all samples were single phase with orthorhombic structure (space group: *Pbnm*) with lattice parameter *a*= 5.496 Å, *b*= 7.703 Å and *c* = 5.471 Å and lattice volume 231.6 $Å^3$. The lattice parameters as shown in Table 1 are almost constant at different sintering temperatures. No peak shift in the XRD patterns was observed, while the relative intensities of the peak changes slightly. This indicated that the sintering temperature does not affect the lattice parameter (Chang et al. 2004) as well as the oxygen contents.

The grain size increased with sintering temperature. When the grain size increased, the grain become more densely packed resulting in narrowing of the grain boundary regions (Figure 2). Higher sintering temperature is expected to yield larger crystallite sizes that reduce the strain as compared to smaller grain size. The same result has been reported in $La_{0.7}Ca_{0.3}MnO_3$ synthesized at 500, 600, 900 and 1300°C (Siwach et al. 2007). In the sample sintered at 1120 °C the larger grains were well separated by smaller grains and the grains do not seem to connect tightly. For samples sintered at 1220 and 1320 °C, well-formed granular crystallites with larger grain size than sample sintered at 1120 °C were observed.

Figure 3 shows the temperature dependence of the resistivity for $La_{0.7}Ca_{0.28}Sr_{0.02}MnO_3$ sintered at 1120, 1220 and 1320 °C, respectively. The T_{im} value was found to increase from 261 K to 271 K with the increase in sintering temperature. The T_{im} for $La_{0.7}Ca_{0.3}MnO_3$ prepared by conventional solid state reaction is around 240.5 K (Jeong et al. 1998) while the one prepared by COP method is around 272 K (Ewe et al. 2008). Insert in Figure 3 shows a linear relationship between the sintering temperature and the insulator-metal transition temperature (T_{im}). In view

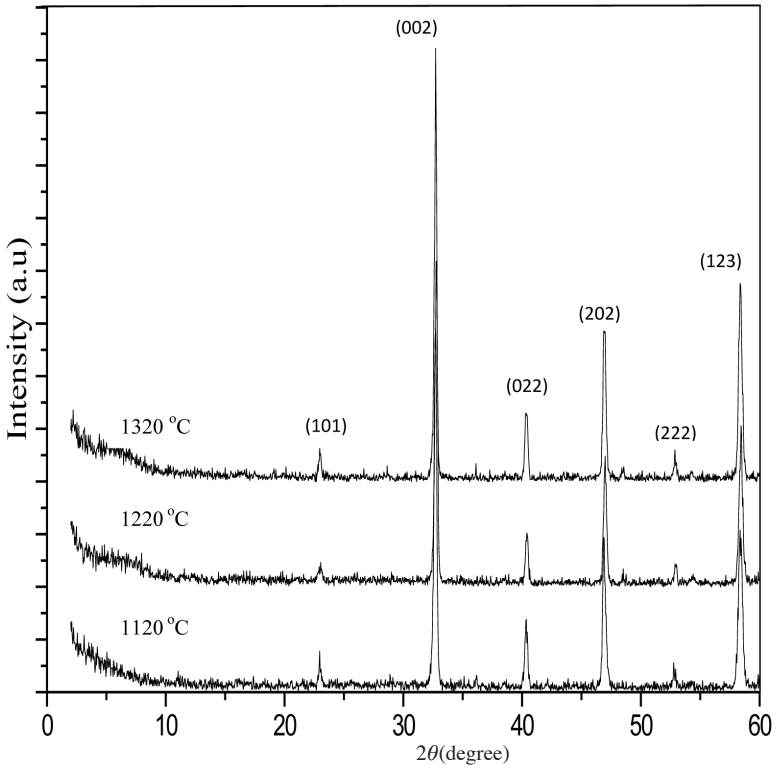

FIGURE 1. X-Ray diffraction patterns of $La_{0.7}Ca_{0.28}Sr_{0.02}MnO_3$ prepared at different sintering temperatures

TABLE 1. Lattice parameters, grain size, T_{im}, density and porosity of $La_{0.7}Ca_{0.28}Sr_{0.02}MnO_3$ at different sintering temperatures

Sintering Temperature (°C)	Lattice parameter (Å) *a*	*b*	*c*	Cell volume ($Å^3$)	Grain size (μm)	T_{im} (K)	Density (ρ_{exp}) (g/cm^3)	Porosity (%)
1120	5.50	7.70	5.47	231.6	18	261	4.64	24.8
1220	5.48	7.77	5.46	232.3	33	266	5.25	15.0
1320	5.46	7.72	5.48	230.7	38	271	5.62	9.00

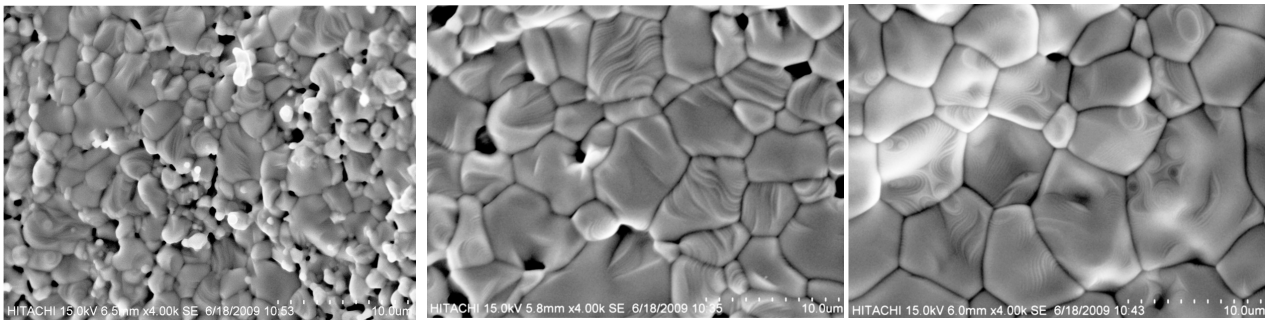

FIGURE 2. Scanning electron micrographs of $La_{0.7}Ca_{0.28}Sr_{0.02}MnO_3$ at different sintering temperatures (a) 1120oC, (b) 1220°C and (c) 1320°C

of this observation, we can say that there is a tremendous influence of grain size on the electrical properties. In sol-gel prepared $La_{0.67}Ca_{0.33}MnO_3$ samples, the decrease in grain size creates a non-magnetic surface layer that has nanocrystalline size around the grains (Venkataiah et al. 2005). This may increase the residual resistivity of the material, which in turns decrease the density of ferromagnetic metallic (FMM) particles, consequently lowering the T_{im} and enhanced the electrical resistivity. Here, the shift of T_{im} towards higher temperature region can

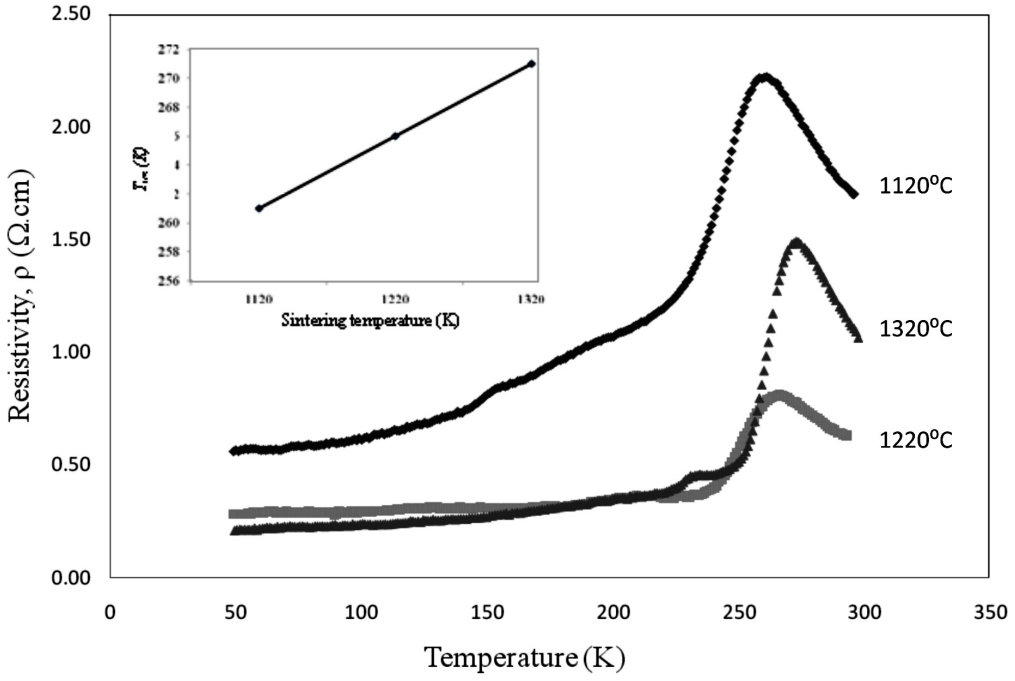

FIGURE 3. Resistivity versus temperature curves of $La_{0.7}Ca_{0.28}Sr_{0.02}MnO_3$ at different sintering temperatures. Insulator-metal transition temperature (T_{im}) versus sintering temperature of $La_{0.7}Ca_{0.28}Sr_{0.02}MnO_3$

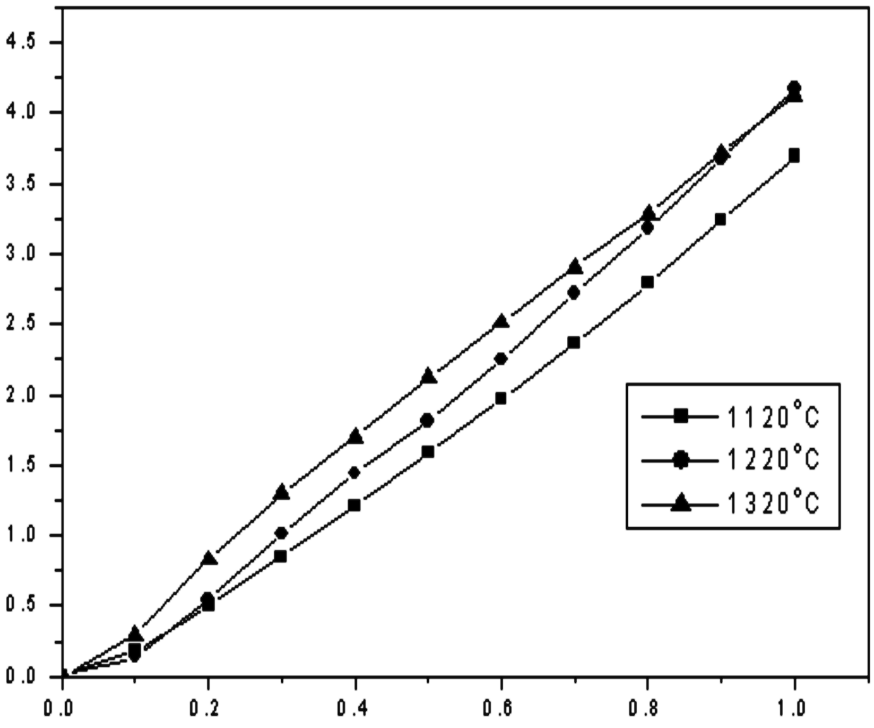

FIGURE 4. Magnetoresistance (%) versus magnetic field (B) of $La_{0.7}Ca_{0.28}$ $Sr_{0.02}MnO_3$ at different sintering temperatures

be explained as due to the enhancement of grain growth that improved the connectivity between the grains and reduced the existing of the pores and voids as shown in Table 1.

A typical plot of percentage of MR versus magnetic field is shown in Figure 4. MR was calculated by using $MR = \frac{\rho_H - \rho_0}{\rho_0} \times 100\%$ (at room temperature). ρ_H is the

TABLE 2. ρ_2, ρ_o, R^2_2 (linear correlation coefficient), $\rho_{2.5}$, ρ_o and $R^2_{2.5}$ of $La_{0.7}Ca_{0.28}Sr_{0.02}MnO_3$ sintered at 1120, 1220, and 1320 °C

Sintering Temperature (°C)	ρ_2 (Ω cm K^{-2})	ρ_o (Ω cm)	R^2_2	$\rho_{2.5}$ (Ω cm $K^{-2.5}$)	ρ_o (Ω cm)	$R^2_{2.5}$
1120	15	0.4583	0.9868	24.8	0.5079	0.9931
1220	1.0	0.2855	0.6754	15.0	0.2880	0.6929
1320	2.8	0.2091	0.9683	9.0	0.2151	0.9762

resistivity measured in the presence of magnetic field and ϱ_o is the resistivity without magnetic field. The percentage of MR for all samples was found to increase with magnetic field. This may be due to the suppression of the magnetic spins scattering with the application of magnetic field, causing the local ordering of the magnetic spins. Due to this ordering, the ferromagnetic metallic (FMM) state suppressed the paramagnetic insulating (PMI) regime. As a result, the conduction electrons (e_g^1) were completely polarized inside the magnetic domain and transferred between the pairs of Mn^{3+} ($t_{2g}^3 e_g^1$:S=2) and Mn^{4+} ($t_{2g}^3 e_g^0$: S=) via oxygen (Venkataiah et al. 2005; Venkataiah et al. 2007).

The weak-links occurred along with the grain growth when the sintering temperature was increased. The reduction of weak-links facilitated the formation of strong intergrain connectivity and enhanced the transport current to flow in bulk matrix. Such connectivity promoted better current percolation between the grains and opens up new conduction channels that do not block the ordering of Mn spins. By decreasing grain size, the spin disorder produced through tunneling process at the grain boundaries and when a magnetic field is applied, the spin disorder is suppressed, resulting in a high MR (Kameli et al. 2008). But results here showed MR at room temperature increased with increase in sintering temperature or grain size (Figure 4). In addition, grains growth with a spiral pattern along a favorable direction has been observed for samples sintered at 1220 and 1320 °C (Figure 2(b) and (c)) but not in sample sintered at 1120 °C. This may be the reason that caused the samples sintered at 1220 °C and 1320 °C to have higher MR (~ 4.2%) compared to sample sintered at 1120 °C (~ 3.8 %). MR value for sample sintered at 1220 and 1320 °C was almost the same. This may be due to the similar grain size of the two samples.

In order to understand the transport mechanisms, we fitted the ρ-T curve according to several models. The electrical resistivity data at low temperatures ($T < T_{im}$) can be fitted to $\rho = \rho_o + \rho_2 T^2$ and $\rho = \rho_o + \rho_{2.5} T^{2.5}$ where ρ_o represents resistivity due to the grain boundary effect, while $\rho_2 T^2$ is due to electron-electron scattering process (Kalyana et al. 2008) and $\rho_{2.5} T^{2.5}$ represents resistivity due to single magnon scattering process in the ferromagnetic phase (Venkataiah et al. 2005). Figure 5(a) and 5(b) shows the resistivity data fitted with $\rho = \rho_o + \rho_2 T^2$ and $\rho = \rho_o + \rho_{2.5} T^{2.5}$. The ρ_2 and $\rho_{2.5}$ values are tabulated in Table 2. As we can see, ρ_o value decreases with an increase in grain size. The enlargement of the grain size may decrease the grain boundary region and hence, the net grain boundary (Ewe et al. 2009). The grain boundary region decreased as a result of an increase in the grain size, which explains why the net grain boundary plays the dominant role in the conduction process. ρ-T^2 and ρ-$T^{2.5}$ curves show that the resistivity data fitted very well as shown by the high linear correlation coefficient value in the ρ-T^2 and ρ-$T^{2.5}$ curves (Table 2). To explain the conduction just above T_{im}, the variable range hopping model are considered while the small polaron hopping is suggested at temperature above $\theta_D/2$ (θ_D is Debye temperature) (Venkataiah et al. 2005).

The activation energy (E_a) and the density of states at the Fermi level ($N(E_F)$) can be calculated from the slope of the graph ln (ρ/T) versus T^{-1} and from the graph ln (ρ) versus $T^{-0.25}$. The activation energy (E_a) and density of states at the Fermi level $N(E_F)$ are shown in Table 3. With an increase in grain size, the interconnectivity between grains increased. This enhanced the possibility of conduction electron to hop to the neighboring sites, thereby decreasing the value of E_a (Venkataiah et al. 2005). The values of E_a for LCSMO in our work also decreased with an increase in grain size. The $N(E_F)$ values were found to increase when the grain size was increased. The $N(E_F)$ reflects the carrier effective mass (or narrowing of the band-width), which in turn results in a drastic change in the resistivity and sharpening of the resistivity peak at the vicinity of T_{im}.

TABLE 3. Pre-factor (ρ_o), activation energy (E_a), T_o and density of states at the Fermi level ($N(E_F)$) of $La_{0.7}Ca_{0.28}Sr_{0.02}MnO_3$ sintered at 1120, 1220, and 1320 °C.

Sintering Temperature (°C)	ρ_o (Ω cm K^{-1})	E_a (meV)	T_o ($\times 10^6$ K)	$N(E_F)$ ($\times 10^{18}$ eV^{-1} cm^{-3})
1120	5.52×10^{-3}	84.4	2.62	3.77
1220	2.03×10^{-3}	65.4	1.49	5.09
1320	1.52×10^{-3}	36.5	0.24	6.57

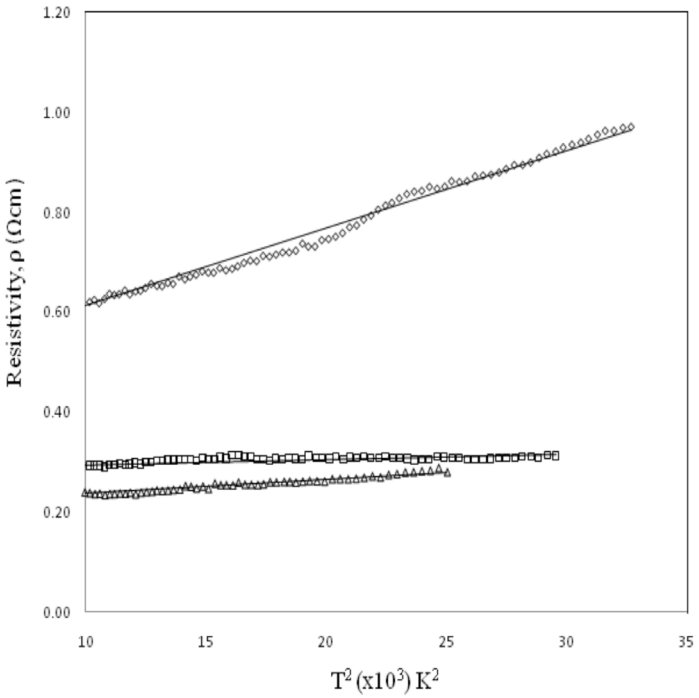

FIGURE 5. Resistivity vs. temperature below T_{im} of $La_{0.7}Ca_{0.28}$ $Sr_{0.02}MnO_3$ with solid line fitted with (a) $\rho = \rho_0 + \rho_2 T^2$ and (b) $\rho = \rho_0 + \rho_{2.5} T^{2.5}$

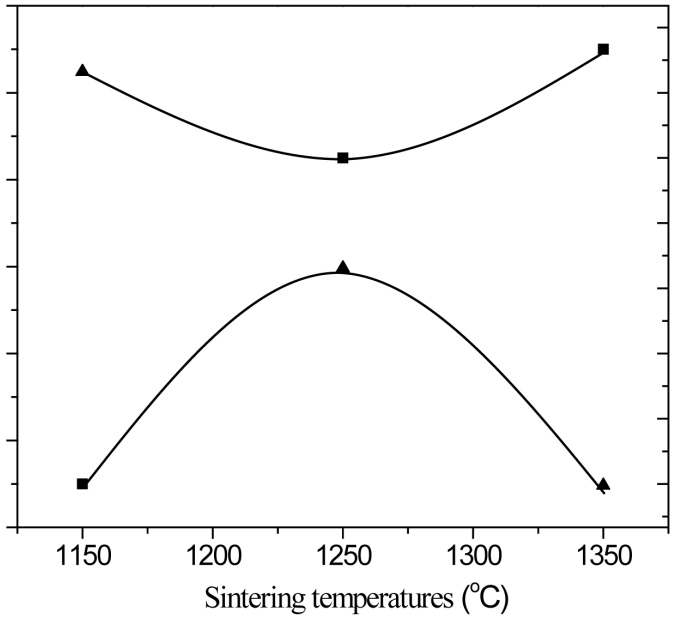

FIGURE 6. T_o and grain size dependence on sintering temperature of $La_{0.7}Ca_{0.28}$ $Sr_{0.02}MnO_3$

Furthermore, as the sintering temperature was increased, T_o values were found to decrease (Table 3). T_o values were also found to be inversely proportional to the grain size (Figure 6), where decreasing in T_o indicates the bending of Mn-O-Mn bond also decreases.

CONCLUSION

In conclusion, the electrical resistivity at low temperature ($T < T_{im}$) regions can be attributed to electron-electron scattering and single magnon scattering process. At high temperature region ($T > T_{im}$), the resistivity may be

explained by the adiabatic small polaron and variable range hopping mechanisms. MR values were found to increase with the increase in magnetic field and sintering temperature at room temperature. Grain growth with a spiral pattern along a favorable direction has enhanced the MR values. The increase of sintering temperature also led to the decrease in the T_o value, where a higher T_o value indicates an increase in the bending of Mn-O-Mn bond angle. Therefore, it may be concluded that the grain growth mechanism affected the electrical, magnetoresistance and magneto-transport properties of the materials. In this paper we reported the properties of $La_{0.7}Ca_{0.33-x}Sr_xMnO_3$ for x = 0.02 with the orthorhombic structure. Further works on higher Sr content and for the rhombohedral structure would give further insights into the materials.

Acknowledgements

This work was supported by the Ministry of Science, Technology and Innovation, Malaysia (SciFund 03-02-03-SF 0217) and Ministry of Higher Education of Malaysia under Fundamental Research grant no. FRGS/FASA 1-2009/SAINS TULEN/UNITEN/104 and UKM-DLP-2011-018.

References

Chang, Y.L. & Ong, C. K. 2004. Temperature sintering effects on the magnetic, electrical and transport properties of $La_{0.67}Sr_{0.33}MnO_3/Nd_{0.67}Sr_{0.33}MnO_3$ composites. *J. Phys Condens. Matter* 16: 3711-3718.

Chattopadhyay, S., Sarkar, A., Pal, S., Kulkarni, S.D., Joy, P.A. & Chaudhari, B. K. 2007. Studies of quenched disorder in $La_{0.7}Ca_{0.3}MnO$-type CMR manganite system from magnetic, transport and positron annihilation spectroscopic measurements. *Physica B* 398: 23-27.

Dagotto, E., Hotta, T. & Moreo, A. 2001. Colossal magnetoresistant materials: The key role of phase separation. *Physics Report* 344: 1-153.

Ewe, L.S., Hamadneh, I., Hazar, A.S. & Abd-Shukor, R. 2008. Sound velocity in perovskite manganites $La_{0.67}Ca_{0.33}MnO_3$ with different grain sizes. *Physica B* 403: 2394-2398.

Ewe, L.S., Hamadneh, I., Salama, H., Nasri, N.A., Halim, S.A. & Abd-Shukor, R. 2009. Magnetotransport properties of $La_{0.67}Ca_{0.33}MnO_3$ with different grain sizes. *Appl. Phys. A* 95: 457-463.

Fontcuberta, J., Martinez, B., Seffar, A., Pinol, S., Garcia-Munoz, J.L. & Obradors, X. 1996. Colossal magnetoresistance of ferromagnetic manganites: Structural tuning and mechanisms. *Phys. Rev. Lett.* 76: 1122-1125.

Grossin, G. & Noudem, J.G. 2004. Synthesis of fine $La_{0.8}Sr_{0.2}MnO_3$ powder by different ways. *Solid State Science* 6: 939-944.

Jeong, Y.H., Park, S.H., Koo, T.Y. & Lee, K.B. 1998. Fisher-Langer relation and scaling in the specific heat and resistivity of $La_{0.7}Ca_{0.3}MnO_3$. *Solid State Ionics* 108: 249-254.

Jin, S. Tiefel, T. H. Mccormack, M. Fastnacht, R. A, Ramesh, R. Chen, H. 1994. Thousand fold change in resistivity in magnetoresistive La-Ca-Mn-O. *Science* 264: 413

Kalyana Lakshmi, Y., Venkataiah, G., Vithal, M. & Venugopal Reddy, P. 2008. Magnetic and electrical behavior of $La_{1-x}A_xMn)_3$ (A= Li, Na, K and Rb) manganites. *Physica B* 403: 3059-3066.

Kameli, P., Salamati, H. & Aezami, A. 2008. Influence of grain size on magnetic and transport properties of polycrystalline $La_{0.8}Sr_{0.2}MnO_3$ manganites. *Journal of Alloys and Compounds* 450: 7-11.

Karmakar, S., Taran, S., Chaudhuri, B.K., Sakata, H., Sun, C.P., Huang, C.L. & Yang, H.D. 2005. Study of grain boundary contribution and enhancement of magnetoreisistance in $La_{0.67}Ca_{0.33}MnO_3/V_2O_5$ composites. *J. Phys. D: Appl. Phys.* 38: 3757-3763.

Rao, C.N. & Raychaudhuri, A.K. 1998. *Colossal Magnetoresistance, Charge Ordering and Other Novel Properties of Manganates and Related Materials*. Singapore: World Scientific.

Ravi, V., Kulkarni, S.D., Samuel, V., Kale, S.N., Mona, J., Rajgopal, R., Daundkar, A., Lahoti, P. S. & Joshee, R. S. 2007. Synthesis of $La_{0.7}Sr_{0.3}MnO_3$ at 800°C using citrate gel method. *Ceramics International* 33: 1129-1132.

Roul, B.K., Sahu, D.R., Mohanty, S. & Pradhan, A.K. 2001. Effect of high temperature sintering schedule for enhanced CMR properties of $La_{0.67}Ca_{0.33}MnO_3$ close to room temperature. *Materials Chemistry and Physics* 67: 267-271.

Siwach, P.K., Prasad, R., Gaur, A., Singh, H.K., Varma, G.D. & Srivastava, O.N. 2007. Microstrcture-magnetotransport correlation in $La_{0.7}Ca_{0.3}MnO_3$. *Journal of Alloys and Compounds* 443: 26-31.

Venkataiah, G., Krishna, D.C., Vithal, M., Rao, S.S., Bhat, S. V., Prasad, V., Subramanyam, S. V. & Venugopal Reddy, P. 2005. Effect of sintering temperature on electrical transport properties of $La_{0.67}Ca_{0.33}MnO_3$. *Physica B* 357: 370-379.

Venkataiah, G. & Venugopal Reddy, P. 2005. Structural, magnetic and magnetotransport behavior of some Nd-based perovskite manganites. *Solid State Communications* 136: 114-119.

Venkataiah, G., Prasad, V. & Venugopal Reddy, P. 2007. Influence of A-site cation mismatch on structural, magnetic and electrical properties of lanthanum manganites. *Journal of Alloys and Compounds* 429: 1-9.

Xiong, C., Hu, H., Xiong, Y., Zhang, Z., Pi, H., Wu, X., Li, L., Wei, F. & Zheng, C. 2009. Electrical properties and enhanced room temperature magnetoresistance in $(La_{0.7}Ca_{0.2}Sr_{0.1}MnO_3)_{1-x}/Pd_x$ composites. *Journal of Alloys and Compounds* 479: 357-362.

Zainullina, Z. I., Bebenin, N. G., Ustinov, V. V. & Mukovskii, Ya. M. 2004. Elastic properties of $La_{1-x}Sr_xMnO_3$ single crystal. *J. Magn. Mag. Mater.* 272-276: e473-e474.

Zhang, Y. B., Li, S., Sun, C. Q., Widjaja, S. & Hing, P. 2006. Transition dependence of $La_{2/3}Ca_{1/3}MnO_3$ oxide on microstructure. *Journal of Materials Processing Technology* 122: 266-271.

L.S. Ewe* & R. Ramli
College of Foundation and General Studies
Universiti Tenaga Nasional
Campus Putrajaya
Jalan Ikram-Uniten 43000 Kajang, Selangor D.E.
Malaysia

K.P. Lim
Physics Department
Faculty of Science
Universiti Putra Malaysia
43400 Serdang, Selangor D.E.
Malaysia

R. Abd-Shukor
School of Applied Physics
Universiti Kebangsaan Malaysia
43600 Bangi, Selangor D.E.
Malaysia

*Corresponding author; email: laysheng@uniten.edu.my

Received: 29 September 2011
Accepted: 16 January 2012